Version of Record: https://www.sciencedirect.com/science/article/pii/S0009261422003049
Manuscript_b5340aff78ba4450055a1bbbdd9b93e6

Mechanism of E-bridge formation by various PAH molecules: A theoretical study

Anna S. Savchenkova[a,*], Alexander S. Semenikhin[a], Ivan V. Chechet[a], Sergey G. Matveev[a], Michael Frenklach[b,*], Alexander N. Morozov[c], and Alexander M. Mebel[a,c,*]

[a] *Samara National Research University, Samara, 443086, Russia. E-mail: paramonovaanna@mail.ru*

[b] *Department of Mechanical Engineering, University of California at Berkeley, Berkeley, California, 94720-1740, USA. E-mail: frenklach@berkeley.edu*

[c] *Department of Chemistry and Biochemistry, Florida International University, Miami, Florida, 33199, USA. E-mail: mebela@fiu.edu*

Abstract

Potential energy surfaces (PES) for dimerization of acepyrene-pyrene, aceanthracene-anthracene, and acenaphthalene-naphthalene were computed by the G3(MP2,CC) and ONIOM2(G3(MP2,CC):B3LYP/6-31G(d)) methods. Close agreement of relative energies of corresponding species along reaction paths for different reactions was found suggesting that the PES for E-bridge formation depends weakly on the number of rings in the interacting monomers. The results indicate that the reaction rate is controlled by the dynamics of the initial collision, which may depend on the monomer size. The ONIOM approach is proposed as an accurate tool for calculations of PES in large PAH systems being more reliable than various DFT methods.

Keywords: polycyclic aromatic hydrocarbons; dimerization mechanism; E-bridge formation; potential energy surface; ONIOM method

Introduction

The process of soot formation is one of the most complex combustion phenomena involving chemical interactions during combustion, heat and mass transfer, gas dynamics and solid particle dynamics at the same time [1]. The key stage for the formation of soot, which is also the least understood and poorly studied, is the nucleation stage [2]. Nucleation is the first stage of the phase transition, where the young soot particles are formed from molecules in the gas phase. Revealing the mechanism and kinetics/dynamics of soot nucleation is critically required for the creation of reliable and predictive kinetic models capable of describing the formation of soot in the smoking flame. This makes the study of the mechanisms of soot nucleation an urgent task.

An early hypothesis for soot nucleation assumed that the transition from gas to solid initiates by irreversible dimerization of middle-size polycyclic aromatic hydrocarbons (PAH), such as pyrene or coronene [3-5]. With this assumption, kinetic models are able to reproduce the development of soot particles in flames numerically [3,6,7], but this assumption appeared to be unjustified due to thermodynamic instability of such mid-size PAH dimers [8-10]. Alternatively, taking much larger PAH molecules as the dimerization precursors cannot reproduce the experimentally observed soot appearance in flames.

A recent publication critically reviewed several alternative proposals for the inception mechanism, including the presence of ions and the formation of chemically-bonded dimers [2]. Although ionic forces tend to heighten PAH clustering (e.g., the addition of alkali-metal ions enhances the formation of small coronene clusters [11] and binding energies of polarized curved PAHs with other PAHs are higher with chemi-ions present in flames [12]), several considerations allowed us to conclude that such a mechanism could not be general [2]. Therefore, we centered on one of the hypotheses for the formation of chemically-bonded dimers that is able to reproduce the rate of nucleation [2]. This mechanism invokes the formation of a dimer of two PAH moieties linked via a so-called E-bridge made of two five-membered rings (or a five- and six-membered rings [13]) adjoined by a common C-C bond, so that two monomers are connected by more than one covalent bond. The E-bridge formation was postulated to be enabled by rotational excitation [2,13] occurring via the development of internal rotation of the colliding monomers. Such a development between two incoming pyrene molecules during their collision, which serves as a temporary energy accumulator for the excess of the collision translational energy slowly dissipating through ro-vibrational energy transfer, was first detected in earlier molecular-dynamics (MD) simulations with on-the-fly semi-empirical quantum (PM3 [14]) forces [15] and recently received further support from the results of a classical trajectory study of pyrene dimerization [16] and from hybrid QM/MM MD simulations by Kraft and co-workers [17]. The existence of a rotationally/vibrationally-excited complex is the keystone of the proposed mechanism since the reaction event in this scenario is the

outcome of the initial encounter of the two PAHs and the overall kinetic rate is determined by the collision rate of the incoming PAHs.

While the details of the proposed rotationally-excited dimerization are being further investigated, in the present study we continue to quantitatively explore the mechanism and potential energy surfaces for the E-bridge formation between PAH monomers increasing in size, from anthracene-aceanthracene to pyrene-acepyrene, with the objective to see if and how the size of the participating monomers affects the energetic parameters of the reaction potential energy surface (PES). In the previous works on E-bridge formation [2,13], we were able to carry out chemically accurate G3(MP2,CC) calculations only for the reactions involving monomers of a relatively small size, acenaphthylene + 1-naphthyl and acenaphthylene + 4-phenanthrenyl, whereas for larger systems like acepyrene + pyrenyl we had to rely on the results of density functional theory (DFT) calculations (B2PLYPD3 [18-20], M06-2X [21], and ωB97XD [22]), since the computational resources needed for a G3(MP2,CC) calculation of such a system are too high. Here, we introduce a variation of the hybrid QM/QM ONIOM method [23] targeting to approximate G3(MP2,CC) energies of larger systems of E-bridge formation, which was successfully employed earlier for the study of HACA growth of large PAH [24]. To establish accuracy of the method, wherever feasible we verify the ONIOM results vs. those from the direct G3(MP2,CC) calculations. In addition, we also consider and analyze a variety of possible reaction pathways to the E-bridge formation and compare the reaction energetics depending on the positions of the attacking radical on the zigzag edge or the front end of the molecule and the attacked C atom in the five-membered ring.

Calculation methods

For reactants, intermediates, transition states, and products, the optimized geometry was calculated, the PES was compiled, and vibrational frequencies were computed using the DFT B3LYP method with the 6-31G(d,p) set of basis functions [25,26]. All DFT calculations were performed using the Gaussian 09 [27] software package. To refine relative energies of various species on the PES for the interaction of acenaphthylene with naphthyl, we employed the MOLPRO 2010 software package [28] to perform calculations using the combined model chemistry G3(MP2,CC) method [29-31], within which the coupled clusters CCSD(T)/6-31G(d) energy is corrected to a larger G3Large basis set using second-order Møller-Plessett perturbation theory MP2 calculations:

$$E[G3(MP2,CC)] = E[CCSD(T)/6\text{-}31G(d)] + E[MP2/G3Large)] - E[MP2/6\text{-}31G(d)] + ZPE[B3LYP/6\text{-}31G(d)] \quad (1)$$

Here, E[MP2/G3Large)] - E [MP2/6-31G(d)] is the basis set correction and ZPE is the zero-point vibrational energy correction computed based on B3LYP/6-31G(d) vibrational frequencies. It is

generally accepted that the B3LYP/6-31G(d,p) method normally provides accuracy within 0.01-0.02 Å for bond lengths and 1-2° for angles for hydrocarbons including PAH molecules and their radicals. In a recent work [32], we checked the performance of the B3LYP method vs. a more recent long-range corrected ωB97XD functional for a PAH growth reaction. The results showed that the B3LYP and ωB97XD optimized geometries were nearly identical and the single-point G3(MP2,CC)//B3LYP and G3(MP2,CC)//ωB97XD relative energies agreed with each other within 0.3 kcal/mol.

With our current computing resources, calculation of G3(MP2,CC) energies in the mechanism of pyrene and anthracene dimerizations requires more than a month for a single structure. Therefore, to achieve a balance between accuracy and timing, we chose to refine the energetics on the corresponding PESs using a less demanding hybrid QM/QM ONIOM approach [23]. In the ONIOM approximation, the energy of a large (real) system under investigation can be represented as a high-level value of the simplified (model) system $E_{high,model}$ corrected with a difference of energies obtained using less costly computational methods for the real system $E_{low,real}$ and the model system $E_{low,model}$:

$$E_{high,real} \approx E_{ONIOM2(high:low)} = E_{high,model} + E_{low,real} - E_{low,model} \quad (2)$$

This ONIOM study employs high-level G3(MP2,CC) energy calculations for the model system and DFT B3LYP/6-31G(d) to compute the system size correction:

$$E_{ONIOM} = E_{G3(CC,MP2),model} + E_{B3LYP,real} - E_{B3LYP,model} \quad (3)$$

This computational scheme is denoted as ONIOM2(G3(MP2,CC)//B3LYP/6-31G(d,p):B3LYP/6-31G(d)). The accuracy of this scheme depends upon the difference between ($E_{low,real} - E_{low,model}$) and ($E_{high,real} - E_{high,model}$) which should be tested for each particular combination of the methods for the chemical system of interest and its partitioning. A similar variation of ONIOM was recently employed to study the HACA growth of large PAH molecules and demonstrated an excellent agreement with the available high-level data [24]. The model systems were chosen in the manner illustrated in Scheme 1: for pyrene-acepyrene, the structures of acepyrene and pyrene each without two aromatic rings that do not participate in the dimerization reaction were selected, whereas for anthracene-aceanthracene, the structures of aceanthracene and anthracene each without one aromatic ring that does not participate in the reaction were chosen. From excluded cycles, the removed C-C bonds were replaced by C-H bonds keeping the same bond angles and dihedral angles as in the real systems with the C-H bond lengths fixed at the typical value for C-H aromatic bonds (1.07 Å). Thus, the structures of the model systems are similar to the naphthyl-acenaphthylene system, but with all interatomic distances in this fragment retained from the real system. For few selected real structures, G3(MP2,CC) calculation were also carried out in order to test the accuracy of the proposed two-layer ONIOM scheme.

It should be noted that the rate limiting step in G3(MP2,CC) calculations is CCSD(T)/6-31G(d). Considering that the CCSD(T) method scales as N^7, where N is the number of basis functions, in going from naphthyl + acenaphthalene (the model system) to pyrenyl + acepyrene (the real system), the required computing time would increase by a factor of $(534/338)^7 = 24.6$, where the numbers in parentheses are the numbers of basis functions for the real and model systems within the 6-31G(d) basis set. Alternatively, within ONIOM calculations the most time-consuming calculation for the real system is B3LYP, which scales as N^4, and so the required time increase with the same 6-31G(d) basis set is only $(534/338)^4 = 6.2$.

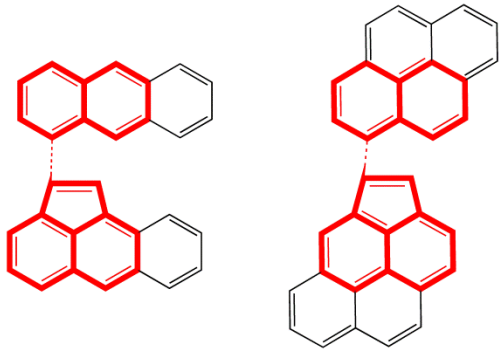

Scheme 1. Model and real systems for the modeling of the anthracene-aceanthracene (left) and pyrene-acepyrene (right) dimerizations. Small (model) systems are shown with bold lines.

Results and discussion

The mechanism of formation of the E-bridge dimer of pyrenyl and acepyrene was described in detail earlier [2], and therefore, for this system, only a brief account of the main results and of refining energy calculations are presented here. The PES for different pathways to form a dimer of pyrene and acepyrene is illustrated in Figure 1. One can see that two dimers, with a 5-5 E-bridge (P1) or a C-C covalent bond (P2), can be produced as a result of the transformation of the W1 intermediate. The easiest way to form this structure is through the addition reaction of pyrenyl to the five-membered ring of acepyrene (R). According to DFT calculations employing various functionals (ωB97XD, M06-2X, and B2PLYPD3), the addition reaction proceeds through a small barrier of 0.3, 2.8, and 1.2 kcal/mol, respectively [2]. Alternatively, the results of the ONIOM calculation suggest a transition state lying 2.8 kcal/mol lower in energy than the reactants, which is associated with the presence of a molecular reactant complex in the entrance channel. This result is actually not surprising because a reactant complex followed by a submerged barrier (with the transition state energy lying under the energies of the reactants) were also found for the naphthyl addition to acenaphthylene at the G3(MP2,CC) level [13]. In the naphthyl-acenaphthylene system, the relative energies of the complex and the transition state were obtained as -2.4 and -1.7 kcal/mol, respectively. Here, for pyrenyl-acepyrene, the submerged transition state energy evaluated using

ONIOM is similar, -2.8 kcal/mol, but the energy of the complex, -13.3 kcal/mol, is likely strongly overestimated in terms of the absolute value. This is supported by the results of the DPLNO-CCSD(T)/cc-pVDZ [33] calculations of the complex and the transition state by the ORCA package [34] giving relative energies of these structures as -3.5 and -2.0 kcal/mol, respectively. Apparently, the present ONIOM combination fails to properly describe the complex long-range binding energy and a caution must be taken when using the ONIOM approach for similar structures. For the products P1 and P2, the differences between ONIOM and G3(MP2,CC) relative energies are 2.4 and 2.0 kcal/mol, respectively. For the intermediates W1 and W2 and transition states for the five-membered ring closure (W1-W2) and H losses (W1-P2 and W2-P1) full G3(MP2,CC) calculations are too demanding and a comparison can only be made with the corresponding structures in the naphthyl-acenaphthylene system [13]. The differences in relative energies do not exceed 1 kcal/mol for the intermediates and 2 kcal/mol for the H loss transition states. However, most likely this deviation is not due to the difference in the methods employed, ONIOM vs. G3(MP2,CC), but is caused by the real chemical difference between the two systems because at the B3LYP level the energies of these TS also differ by the similar value.

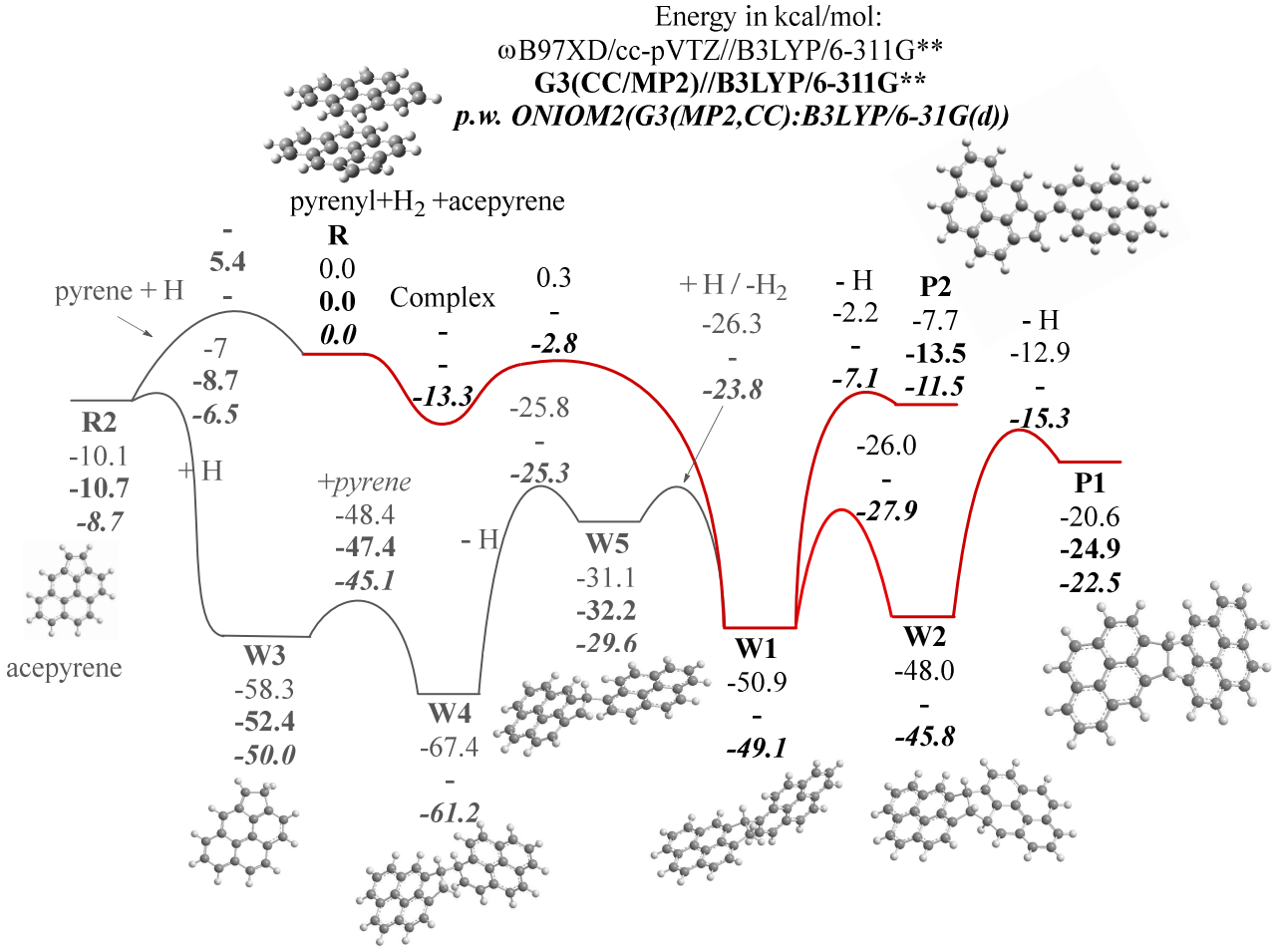

Figure 1. Potential energy surface for the E-bridge formation of pyrene and acepyrene.

The second, less feasible path to the formation of W1 is associated with the initial formation of the H-acepyrenyl radical W3 through H addition to the five-membered ring in acepyrene, the addition of pyrene to W3, and the transformation of the resulting structure W4 via unimolecular H loss followed bimolecular H abstraction, e.g. by an H atom. The H-acepyrenyl radical is formed as a result of the addition of hydrogen to the five-membered acepyrene ring through a small barrier of 2.2 kcal/mol at the ONIOM level of theory. The energy of the products relative to the reactants is -50.0 kcal/mol. The subsequent addition of pyrene proceeds through a barrier of 4.9 kcal/mol and forms the W4 structure with a relative energy of -61.2 kcal/mol. The conversion of W4 to W1 involves a hydrogen elimination step and a direct hydrogen abstraction step. The H atom loss step from W4 proceeds through a barrier of 35.9 kcal/mol and leads to the formation of W5 with a relative energy of -29.6 kcal/mol. W5 can be converted to W1 by abstraction of a hydrogen atom by another hydrogen atom. This reaction proceeds through a barrier of 5.9 kcal/mol and makes the W1 + H_2 product with an energy of -49.1 and -40.4 kcal/mol relative to the reactants R and R2, respectively. The P2 dimer with a covalent C-C bond is formed as a result of the hydrogen elimination from the five-membered ring through a barrier of 42.0 kcal/mol, the energy of the products is -11.5 kcal/mol relative to R. The transformation of W1 with the formation of the second five-membered ring in W2 proceeds through a barrier of 21.2 kcal/mol and is more favorable. The energy of W2 is 45.8 kcal/mol lower than that of the pyrenyl + acepyrene reactants R. The subsequent loss of the hydrogen atom from W2 with the formation of the 5-5 E-bridge structure proceeds through a barrier of 30.5 kcal/mol, the energy of the product is 22.5 kcal/mol lower than the energy of R. It should be noted that our previous kinetic calculations have shown that the pathway to W1 (and hence to the E-bridge dimer P1) initiated by H addition to acepyrene (to W3) and followed by pyrene addition to H-acepyrenyl (to W4) is unfavorable under typical combustion conditions because first, the H-acepyrenyl radical is unstable with respect to H loss at temperatures above ~1250 K (at 1 atm) and hence is unlikely to enter a bimolecular reaction with pyrene, and second, the W3 + pyrene $\rightarrow$ W5 + H reaction is much faster in the reverse direction than in the forward one; we refer the reader to the previous work [2] for a more detailed analysis. Thus, only the pyrenyl + acepyrene pathway is really relevant to the E-bridge formation.

Nevertheless, the present calculations allowed us to test the accuracy of the ONIOM scheme with respect to G3(MP2,CC) for a broader range of structures. The results of the ONIOM calculations are in good agreement with the available G3(MP2,CC) data. For instance, the average unsigned difference between the values obtained by the two methods is 2.3 kcal/mol and the largest deviation is 2.6 kcal/mol for W5. Moreover, the ONIOM method systematically overestimates the relative energies of all species with respect to R by ~2 kcal/mol. Thus, ONIOM calculations provide reasonably accurate results using significantly less computing resources. The deviations between

the relative energies in the pyrene/acepyrene dimerization system computed by any of the DFT methods used (B3LYP, ωB97XD, M06-2X, or B2PLYPD3) are significantly larger (see Fig. 5 in [2]) and are not systematic. Therefore, we expect that the ONIOM2(G3(MP2,CC):B3LYP/6-31G(d)) approach should be a much more reliable tool for energy evaluation in larger systems than the DFT methods tested so far.

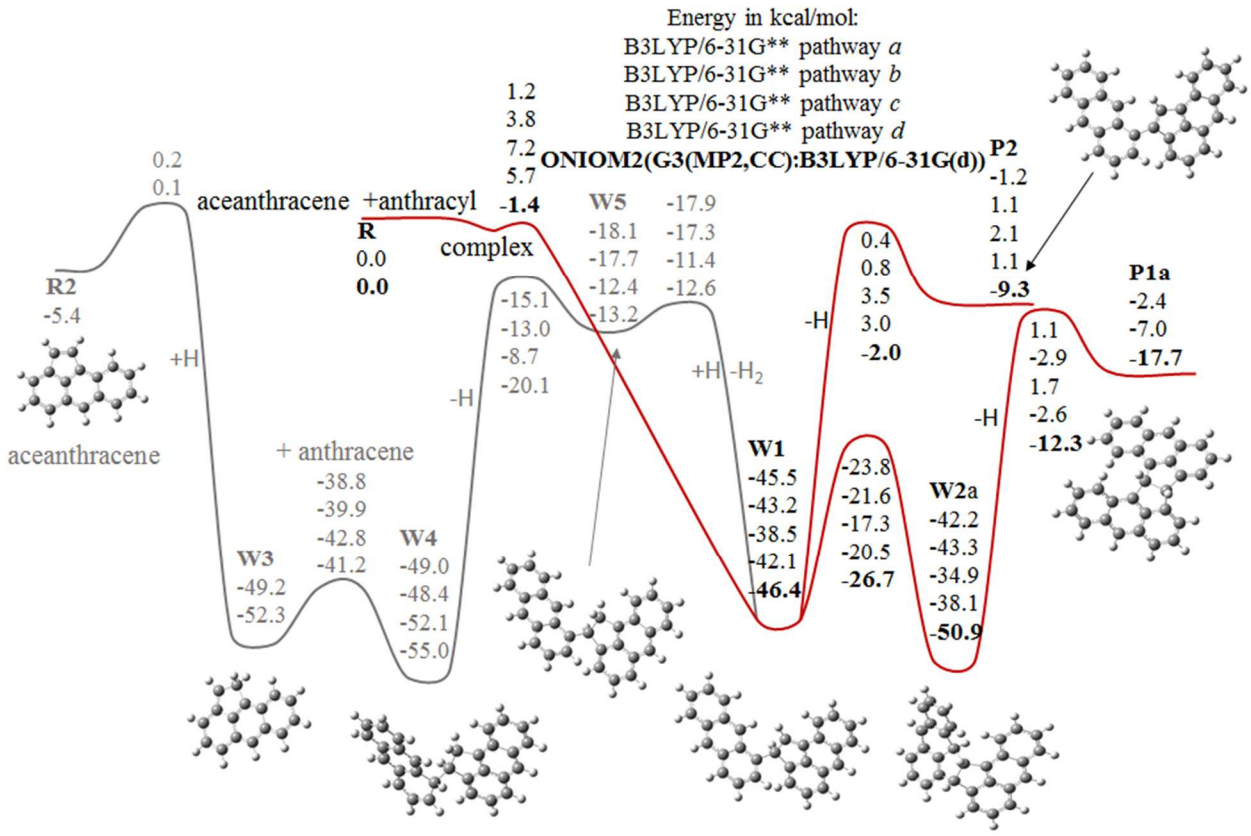

Figure 2. Potential energy surface for E-bridge formation of anthracene and aceanthracene.

For the aceanthracene-anthracene system (Figure 2), the reaction mechanism of the formation of E-bridge dimers is similar to that considered above for acepyrene-pyrene. Since it was shown earlier [2] that for the dimerization of acepyrene with pyrene the most important reaction path is the reaction of acepyrene and pyrenyl, the ONIOM method was used only for the analogous aceanthracene + anthracenyl channels, while for the H-aceanthacenyl + anthracene pathways we limited our consideration only to B3LYP calculations. In addition, there is another significant difference in the aceanthracene-anthracene system as compared to acenaphthylene-naphthalene and acepyrene-pyrene. The attachment of pyrene and acepyrene, naphthalene and acenaphthalene to one another can proceed in one and only way. On the contrary, for the aceanthracene-anthracene system, several variations are possible. After an H atom abstraction from the zigzag edge of anthracene two distinct radicals can be formed, 1- and 9-anthracenyl. Then, the addition of the aceanthracene molecule can take place in positions 1 and 2 (Scheme 2). This leads to the possibility of the formation of four variants of the intermediate W1, differing in the arrangement of benzene

rings relative to each other. Further transformation of W1 also proceeds in four variations, eventually leading to four variants of the P2 product and two variants of the P1 product. As can be seen from the calculated PES in Fig. 2, the difference in the relative energies of the intermediates and transition states for the considered variations does not usually exceed, 7 kcal/mol. The exception is the W4-W5 transition, for which the difference between the variants *c* and *d* is 12.4 kcal/mol, but this pathway is not important for the dimerization process. Considering that the differences in energies for different pathways are not large, pathway *a* was chosen to refine the energies by the ONIOM method, and it was assumed that for the other three pathways the energies and reaction rate constants would be comparable to those obtained for the pathway *a*.

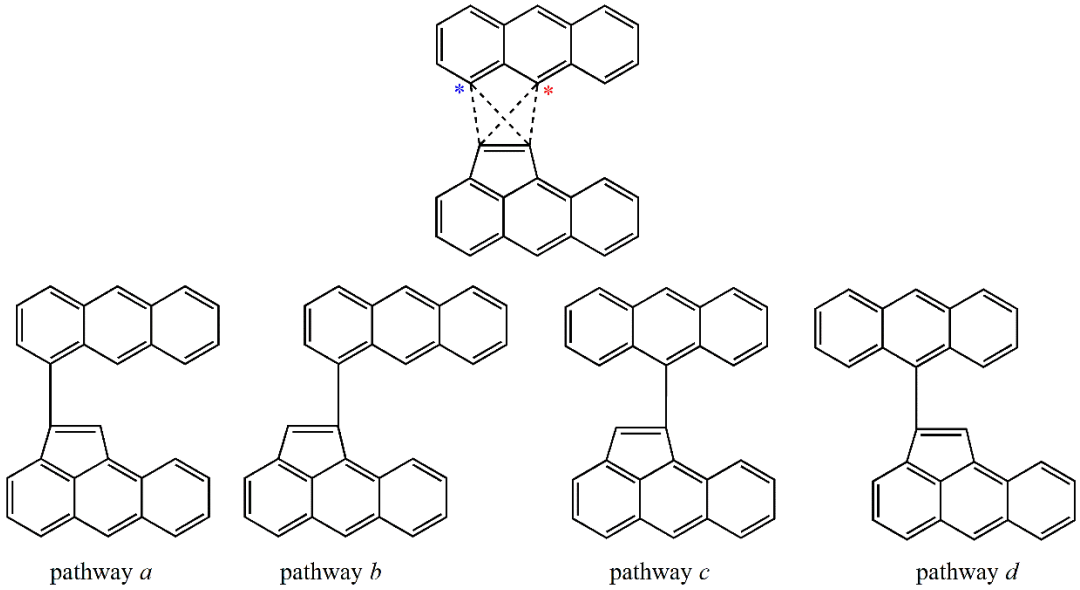

Scheme 2. Possible pathways for the addition of anthracenyl radicals to aceanthracene (top) and four variants of the intermediate W6, which can be formed by the dimerization anthracene with aceanthracene (bottom).

Summarizing the most favorable reaction mechanism, anthracenyl adds to aceanthracene via a submerged barrier (-1.4 kcal/mol) producing a covalently bound complex W1 stabilized by 46.4 kcal/mol. The latter can either lose an H atom forming P2 (-9.3 kcal/mol) via a transition state located 2.0 kcal/mol below the initial reactants or undergo closure of a five-membered ring (E-bridge formation) via a TS at -26.7 kcal/mol producing W2 (-50.9 kcal/mol). Intermediate W2 then decomposes to the E-bridge product P1 (-17.7 kcal/mol) via a TS at -12.3 kcal/mol.

The formation of the E-bridge dimer from 1-naphtyl and acenaphthylene was investigated by the G3(CC,MP2)//B3LYP/6-311G(d,p) method in [13]. The PES was expanded here and is presented in Figure 3. As can be seen from the figure, the PES for this reaction is similar to those considered above for the acepyrene-pyrene and aceanthracene-anthracene systems. It should be noted that TS for the five-member closure ring W1-W2 reported in the earlier work [13] has a higher energy than that of the alternative TS for the same reaction step we found here. The new

TS(W1-W2) is consistent in terms of its energetics and structure with the analogous TS in the anthracene-aceanthracene and pyrene-acepyrene systems.

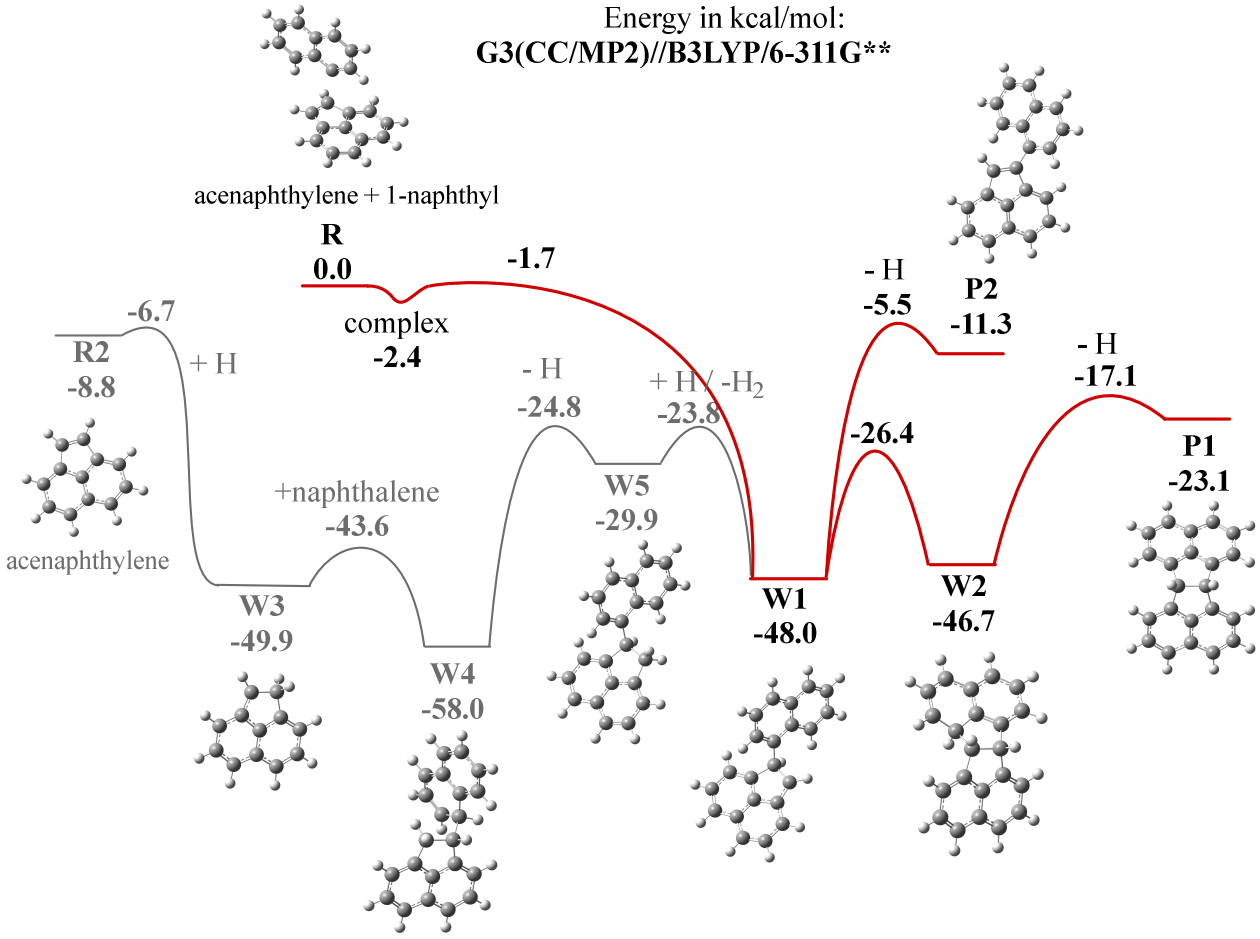

Figure 3. Potential energy surface of E-bridge formation of naphthalene and acenaphthylene.

Table 1. Relative energies (kcal/mol) of various structures on the pathway to the formation of PAH dimers from a PAH radical and ace-PAH calculated at the G3(MP2,CC) and ONIOM2(G3(MP2,CC):B3LYP/6-31G(d)) levels of theory.

	naphthyl-acenaphthalene	anthracenyl-anthracene	pyrenyl-acepyrene	
Structure	G3(MP2,CC)	ONIOM	G3(MP2,CC)	ONIOM
TS R-W1	-1.7	-1.4		-2.8
W1	-48.0	-46.4		-49.1
TS W1-P2	-5.5	-2.0		-7.1
P2	-11.3	-9.3	-13.5	-11.5
TS W1-W2	-26.4	-26.7		-27.9
W2	-46.7	-50.9		-45.8
TS W2-P1	-17.1	-12.3		-15.3
P1 (E-bridge)	-23.1	-17.7	-24.9	-22.5

A comparison of the PESs of different reactions considered here (Table 1) shows that, in general, the surfaces for all three systems are in rather close agreement with each other and thus, the

effects of the environment of the active reaction site on the mechanism and energetics are relatively small. For the reaction products (P1 and P2) and transition states leading to these products (W2-P1 and W1-P2), the relative energies are slightly higher for the aceanthracene-anthracene system than for naphthalene-acenaphthylene and pyrene-acepyrene. The largest difference is observed for the E-bridge dimer and amounts to 5.4 kcal/mol, which could be due to a more favorable interaction between benzene rings of the monomer. This result may indicate that larger linear acenes may have a lower propensity to form E-bridge dimers than pyrene-like PAH. For other intermediates and transition states, comparable values of relative energies are observed, the difference for the considered systems does not exceed 1.2 kcal/mol, where the results of the G3(MP2,CC) and ONIOM methods were compared.

Conclusions

A comparative analysis of PES for dimerization in three systems, acepyrene-pyrene, aceanthracene-anthracene, and acenaphthalene-naphthalene, showed a close agreement of the relative energies of various species along the reaction paths, which suggests that the PES for the E-bridge formation reactions only weakly depend on the number of rings in the interacting monomer molecules. In the meantime, our results indicate that larger linear acenes may have a lower propensity to form E-bridge dimers than pyrene-like PAH. Since all intermediates, transition states, and products in the reactions of an aryl radical with an ace-arene lie lower in energy than the reactants, we anticipate that the reaction rate is controlled by the dynamics of the initial collision, which in turn may depend on the size of the interacting monomers.

From the methodical point of view, the present calculations demonstrate that the ONIOM approach provides relative energies of various species on the dimerization pathways of PAH molecules that are comparable in accuracy to those obtained by the G3(MP2,CC) method, but with a significant reduction of the required computer time and resources. On the contrary, the deviations between the relative energies in the considered dimerization systems computed by the DFT methods are more significant and do not behave systematically. The ONIOM2(G3(MP2,CC):B3LYP/6-31G(d)) method is hence proposed as a reasonably reliable tool for energy calculations of PES in large PAH systems.

Acknowledgements

The work at Samara University was supported by the grant from the Russian Science Foundation (project No. 19-73-00316). The work at Florida International University was funded by the US Department of Energy, Basic Energy Sciences DE-FG02-04ER15570.

References

1. H. Wang, Formation of nascent soot and other condensed-phase materials in flames, Proc. Combust. Inst. 33 (2011) 41–67.
2. M. Frenklach, A.M. Mebel, On the mechanism of soot nucleation , Phys. Chem. Chem. Phys. 22 (2020) 5314-5331.
3. M. Frenklach, H. Wang, Detailed modeling of soot particle nucleation and growth, Proc. Combust. Inst. 23 (1991) 1559–1566.
4. M. Frenklach, An International Round Table Discussion, in: H. Jander, H. G. Wagner (Eds.), Soot Formation in Combustion: Göttingen, 1989, pp. 35–36.
5. M. Frenklach, H. Wang, Detailed mechanism and modeling of soot particle formation, in: H. Bockhorn (Ed.), Soot Formation in Combustion: Mechanisms and Models, Springer-Verlag, Heidelberg, 1994, pp. 165–192.
6. J. Appel, H. Bockhorn, M. Frenklach, Kinetic modeling of soot formation with detailed chemistry and physics: Laminar premixed flames of C_2 hydrocarbons. Combust. Flame 121 (2000) 122–136.
7. D. Hou, C. S. Lindberg, M. Y. Manuputty, X. You, M.Kraft, Modelling soot formation in a benchmark ethylene stagnation flame with a new detailed population balance model. Combust. Flame 203 (2019) 56-71.
8. H. Sabbah, L. Biennier, S. J. Klippenstein, I. R. Sims, B. R. Rowe, Exploring the role of PAHs in the formation of soot: Pyrene dimerization. J. Phys. Chem. Lett. 1 (2010) 2962-2967.
9. P. Elvati, A. Violi, Thermodynamics of poly-aromatic hydrocarbon clustering and the effects of substituted aliphatic chains. Proc. Combust. Inst. 34 (2013) 1837-1843.
10. A. Menon, J. W. Martin, J. Akroyd, M. Kraft, Reactivity of polycyclic aromatic hydrocarbon soot precursors: Kinetics and equilibria. J. Phys. Chem. A 124 (2020) 10040-10052.
11. M. Bartolomei, F. Pirani, J. M. C. Marques, Aggregation enhancement of coronene molecules by seeding with alkali-metal ions. Phys. Chem. Chem. Phys. 21 (2019) 16005-16016.
12. K. Bowal, J. W. Martin, A. J. Misquitta, M. Kraft, Ion-induced soot nucleation using a new potential for curved aromatics, Combust. Sci. Technol. 191 (2019) 747-765.
13. A. S. Semenikhin, A. S. Savchenkova, I. V. Chechet, S. G. Matveev, M. Frenklach, A. M. Mebel, On the mechanism of soot nucleation. II. E-bridge formation at the PAH bay. Phys. Chem. Chem. Phys. 22 (2020) 17196-17204.

14. J. J. P. Stewart, Optimization of parameters for semiempirical methods I. Method. J. Comput. Chem. 10 (1989) 209-220.
15. C. A. Schuetz, M. Frenklach, Nucleation of soot: Molecular dynamics simulations of pyrene dimerization. Proc. Combust. Inst. 29 (2003) 2307-2314.
16. D. Chakraborty, H. Lischka, W. L. Hase, Dynamics of pyrene-dimer association and ensuing pyrene-dimer dissociation. J. Phys. Chem. A 124 (2020) 8907-8917.
17. J. W. Martin, L. Pascazio, A. Menon, J. Akroyd, K. Kaiser, F. Schulz, M. Commodo, A. D'Anna, L. Gross, M. Kraft, π-Diradical Aromatic Soot Precursors in Flames. J. Am. Chem. Soc. 143 (2021) 12212-12219.
18. S. Grimme, Semiempirical hybrid density functional with perturbative second-order correlation, J. Chem. Phys., 124 (2006) 034108.
19. L. Goerigk, S. Grimme, Efficient and accurate doublehybrid-meta-GGA density functionals—evaluation with the extended GMTKN30 database for general main group thermochemistry, kinetics, and noncovalent interactions, J. Chem. Theory Comput. 7 (2011) 291–309.
20. S. Grimme, S. Ehrlich, L. Goerigk, Effect of the damping function in dispersion corrected density functional theory, J. Comput. Chem. 32 (2011) 1456–1465.
21. Y. Zhao, D. G. Truhlar, Density functionals with broad applicability in chemistry, Acc. Chem. Res. 41 (2008) 157–167.
22. J.-D. Chai, M. Head-Gordon, Long-range corrected hybrid density functionals with damped atom-atom dispersion corrections, Phys. Chem. Chem. Phys. 10 (2008) 6615–6620.
23. L. W. Chung, W. M. C. Sameera, R, Ramozzi, A. J. Page, M. Hatanaka, G. P. Petrova, T. V. Harris, X. Li, Zh. Ke, F. Liu, H.-B. Li, L. Ding, K. Morokuma, The ONIOM Method and Its Applications, Chem. Rev. 115 (2015) 5678−5796.
24. A. Chengcheng, R. Shanshan, H. Wei, L. Yi, H. Chenliang, X. Kangwei, Zh. Lidong, Toward high-level theoretical studies on the reaction kinetics of PAHs growth based on HACA pathway: An ONIOM[G3(MP2,CC)//B3LYP:DFT] method developed. Fuel 301 (2021) 121052.
25. C. Lee, W. Yang, R. G. Parr, Development of the Colle-Salvetti correlation-energy formula into a functional of the electron density, Phys. Rev. B 37 (1988) 785–789.
26. A. D. Becke, Density-functional thermochemistry. III. The role of exact exchange, J. Chem. Phys. 98 (1993) 5648–5652.
27. M. J. Frisch, G. W. Trucks, H. B. Schlegel, G. E. Scuseria, M. A. Robb, J. R. Cheeseman, G. Scalmani, V. Barone, B. Mennucci, G. A. Petersson, H. Nakatsuji, M. Caricato, X. Li, H. P. Hratchian, A. F. Izmaylov, J. Bloino, G. Zheng, L. Sonnenberg, M. Hada, M. Ehara, K.

Toyota, R. Fukuda, J. Hasegawa, M. Ishida, T. Nakajima, Y. Honda, H. Nakai, T. Vreven, J. A. Montgomery, J. E. Peralta, F. Ogliaro, M. Bearpark, J. J. Heyd, E. Brothers, K. N. Kudin, V. N. Staroverov, T. Keith, R. Kobayashi, J. Normand, K. Raghavachari, A. Rendell, J. C. Burant, S. S. Iyengar, J. Tomasi, M. Cossi, N. Rega, J. M. Millam, M. Klene, J. E. Knox, J. B. Cross, V. Bakken, C. Adamo, J. Jaramillo, R. Gomperts, R. E. Stratmann, O. Yazyev, A. J. Austin, R. Cammi, C. Pomelli, J. W. Ochterski, R. L. Martin, K. Morokuma, V. G. Zakrzewski, G. A. Voth, P. Salvador, J. J. Dannenberg, S. Dapprich, A. D. Daniels, O. Farkas, J. B. Foresman, J. V. Ortiz, J. Cioslowski and D. J. Fox, Gaussian 09, 2010

28. H.-J. Werner, P. J. Knowles, G. Kinizia, F. R. Manby, M. Schutz, P. Celani, T. Korona, R. Lindh, MOLPRO, 2010.
29. A. G. Baboul, L. A. Curtiss, P. C. Redfern, K. Raghavachari, Gaussian-3 theory using density functional geometries and zero-point energies, J. Chem. Phys. 110 (1999) 7650–7657.
30. L. A. Curtiss, P. C. Redfern, K. Raghavachari, V. Rassolov, J. A. Pople, Gaussian-3 theory using reduced Møller-Plesset order, J. Chem. Phys. 110 (1999) 4703–4709.
31. L. A. Curtiss, K. Raghavachari, P. C. Redfern, A. G. Baboul, J. A. Pople, Gaussian-3 theory using coupled cluster energies, Chem. Phys. Lett. 314 (1999) 101–107.
32. G. R. Galimova, I. A. Medvedkov, A. M. Mebel, The role of methylaryl radicals in the growth of polycyclic aromatic hydrocarbons: The formation of five-membered rings, J. Phys. Chem. A 126 (2022) 1233-1244.
33. R. Christoph, S. Barbara, H. Andreas, N. Frank, Natural triple excitations in local coupled cluster calculations with pair natural orbitals, J. Chem. Phys. 139 (2013) 134101.
34. N. Frank, W. Frank, B. Ute, R. Christoph, The ORCA quantum chemistry program package, J. Chem. Phys. 152 (2020) 224108.

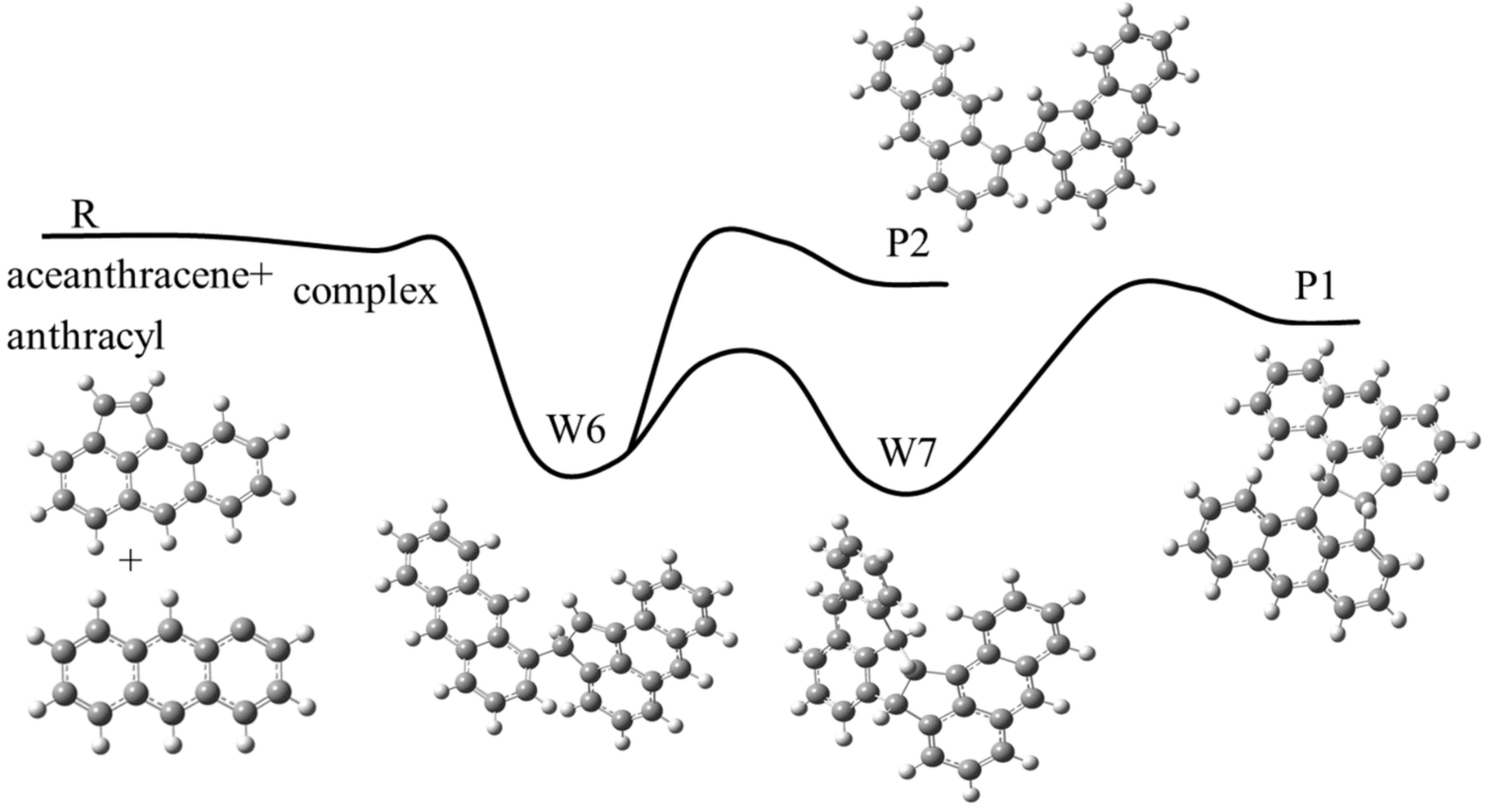
R
aceanthracene+
anthracyl
+
complex
W6
W7
P2
P1